

Ba(Zn_{1-2x}Mn_xCo_x)₂As₂: A Bulk Form Diluted Magnetic Semiconductor with n-type Carriers

Huiyuan Man¹, Cui Ding¹, Shengli Guo¹, Guoxiang Zhi¹, Xin Gong¹, Quan Wang¹, Hangdong Wang², Bin Chen², F.L. Ning^{1,*}

¹*Department of Physics, Zhejiang University, Hangzhou 310027, China and*

²*Department of Physics, Hangzhou Normal University, Hangzhou 310016, China*

(Dated: March 18, 2014)

Abstract

We report the synthesis and characterization of bulk form diluted magnetic semiconductors Ba(Zn_{1-2x}Mn_xCo_x)₂As₂ ($0 \leq x \leq 0.15$) with a crystal structure identical to that of 122-type Fe-based superconductors. Mn and Co co-doping into the parent compound BaZn₂As₂ results in a ferromagnetic ordering below $T_C \sim 80$ K. Hall effect measurements indicate that the carrier are n-type with the density of $\sim 10^{17}/\text{cm}^3$. The common crystal structure and excellent lattice matching between the p-type ferromagnetic Ba_{1-y}K_y(Zn_{1-x}Mn_x)₂As₂, the n-type ferromagnetic Ba(Zn_{1-2x}Mn_xCo_x)₂As₂, the antiferromagnetic BaMn₂As₂ and the superconducting Ba(Fe_{1-x}Co_x)₂As₂ systems make it possible to make various junctions between these systems through the As layer.

PACS numbers: 75.50.Pp, 71.55.Ht, 76.75.+i

*Electronic address: ningfl@zju.edu.cn

The research into diluted magnetic semiconductors (DMS) has been explosive since the observation of ferromagnetic ordering in III-V (Ga,Mn)As thin-film by Ohno et al [1][2–4]. After almost 20 years of efforts, the highest Curie temperature, T_C , has been reported as ~ 200 K with Mn doping levels of $\sim 12\%$ in (Ga,Mn)As [5, 6]. It has been proposed theoretically that the application of spintronics will become possible once T_C reaches room temperature [4]. Improving T_C is, however, hindered by an inherent difficulty: the mismatch of valences of Ga^{3+} and Mn^{2+} prohibits the fabrication of bulk form specimens and homogeneous thin films with higher Mn doping levels. On the other hand, Mn substitution for Ga not only acts as a local moment, but also donates a hole, i.e., p-type carriers. Furthermore, some Mn impurities enter interstitial sites, which makes it difficult to determine precisely the amount of Mn that substitutes Ga [2]. The absence of decisive determination of the actual amount of Mn that substituted Ga also makes it difficult to measure where holes reside in: the impurity band or the valence band [7].

Prior to the research of (Ga,Mn)As, a large group of II-VI family of DMS have also been extensively studied. Because Mn ions have the same valence as that of Zn ions, the chemical solubility can be very high, i.e., $\sim 70\%$ in $(\text{Zn}_{1-x}\text{Mn}_x)\text{Se}$ [8, 9], and bulk form specimens are available. However, it is difficult to control the carrier density, which is as low as 10^{17} cm^{-3} , and the type of carriers [10, 11]. The magnetic moment size is as small as $0.01 \mu_B/\text{Mn}$ in most II-VI DMS [9, 12]. In general, the ground state is believed to be a spin-glass, instead of a long range ferromagnetic ordering.

An pioneer theoretical work proposed by Masek et al has shown that the I-II-V direct-gap semiconductor LiZnAs is a good candidate for fabrication of next generation of DMS [13]. LiZnAs is a direct gap semiconductor with a band gap of 1.6 eV [14–17]. It has a cubic structure, similar to that of zinc-blende GaAs and ZnSe. More interestingly, if we view the combination of $(\text{Li}^{1+}\text{Zn}^{2+})$ as Ga^{3+} , (LiZn)As becomes GaAs; alternatively, if we view the combination of $(\text{Li}^{1+}\text{As}^{3-})$ as Se^{2-} , Zn(LiAs) becomes ZnSe. From the view of synthesis: The I-II-V semiconductor LiZnAs has two superior advantages over III-V and II-VI semiconductors: (1) the isovalent substitution of Mn for Zn overcomes the small chemical solubility encountered in (Ga,Mn)As; (2) the carrier type and density can be controlled by off-stoichiometry of Li concentrations, i.e., extra Li introduce electrons and Li deficiency bring holes.

Recently, Deng et al. successfully synthesized two bulk I-II-V DMS systems, $\text{Li}(\text{Zn,Mn})\text{As}$

[18] and Li(Zn,Mn)P [19], with $T_C \sim 50$ K. It has been shown by muon spin relaxation (μ SR) and nuclear magnetic resonance (NMR) that Mn atoms are homogenously doped into the compound, and the ferromagnetic ordering is truly arising from the Mn atom that substituted into the ionic Zn sites, not from magnetic impurities or clusters. The I-II-V DMSs have advantages of decoupling spins and carriers, where spins are introduced by Mn atoms and carriers are created by off-stoichiometry of Li concentrations. This advantage makes it possible to precisely control the amount of spins and carriers, and investigate their individual effects on the ferromagnetic ordering. The puzzle in Li(Zn,Mn)As and Li(Zn,Mn)P DMS, however, is that the carrier is always p-type even excess Li are introduced during the synthesis process. This is in contrast with the intuitive expectation that excess Li will render a *n*-type carriers. There are no convincing experiments to clarify this issue so far. Based on first-principles calculations, Deng et al [19] shows that excess Li^{1+} ions are thermodynamically favored to occupy the Zn^{2+} sites, and each Li^{1+} substitution for Zn^{2+} will introduce a hole carrier.

Very recently, several more bulk DMS systems with decoupling spins and charges have been reported. Firstly, Ding et al [20] and Han et al [21] reported the ferromagnetic ordering below $T_C \sim 40$ K in “1111” type (La,Ba)(Zn,Mn)AsO and (La,Ca)(Zn,Mn)SbO systems; and Yang et al reported the fabrication of another “1111” type DMS (La,Sr)(Cu,Mn)SO with $T_C \sim 210$ K [22]. Secondly, Zhao et al. reported the “122” type DMS systems, (Ba,K)(Zn,Mn) $_2$ As $_2$, which has T_C as high as 180 K [23], and Yang et al observed the ferromagnetic transition below $T_C \sim 17$ K and a large negative magnetoresistance in (Ba,K)(Cd,Mn) $_2$ As $_2$ [24]. It is worth to note that the Curie temperature of (La,Sr)(Cu,Mn)SO and (Ba,K)(Zn,Mn) $_2$ As $_2$ polycrystals is already comparable to the record T_C of (Ga,Mn)As thin films [5, 6]. Interestingly, the type of carriers in above bulk form DMSs are all p-type, and no n-type DMS has been achieved.

In this letter, we report the synthesis and characterization of Mn and Co co-doped Ba(Zn $_{1-2x}$ Mn $_x$ Co $_x$) $_2$ As $_2$ ($0 \leq x \leq 0.15$) semiconductors. We found that Mn and Co co-doping into the parent compound BaZn $_2$ As $_2$ results in a ferromagnetic ordering below $T_C \sim 80$ K. The coercive field is in the order of ~ 200 Oe, which is comparable to that of the cubic (Ga,Mn)As, Li(Zn,Mn)As and Li(Zn,Mn)P. The electrical transport measurements show typical semiconducting behavior. Hall effect measurements indicate that the carrier are n-type with the density of $\sim 10^{17}/\text{cm}^3$. We found that doping Co alone results in some

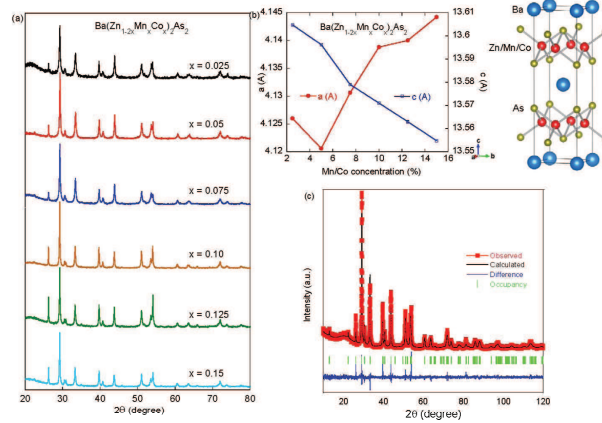


FIG. 1: (Color online). (a) The X-ray diffraction patterns of $\text{Ba}(\text{Zn}_{1-2x}\text{Mn}_x\text{Co}_x)_2\text{As}_2$ ($0 \leq x \leq 0.15$). (b) The systematic change of the lattice constants a and c . The crystal structure is shown, which is isostructural to 122 Fe-based superconductors. (c) The XRD diffraction peaks can be well indexed into the tetragonal structure of space group $I4/mmm$.

type of magnetic ordering with a much smaller saturation moment size. Only co-doped with Mn atoms, a ferromagnetic ordering with saturation moment size of $\sim 0.1 \mu\text{B}/\text{TM}$ (TM = Mn, Co) is observed.

We synthesized the polycrystalline specimens $\text{Ba}(\text{Zn}_{1-2x}\text{Mn}_x\text{Co}_x)_2\text{As}_2$ ($x = 0.025, 0.05, 0.075, 0.10, 0.125, 0.15$) by the solid state reaction method. Zn (99.9%), Mn (99.99%), Co (99.99%) and As (99%) were sintered at 800° for 10 hours to make the precursors ZnAs, MnAs and CoAs. Then the mixture of Ba (99.9%), ZnAs, MnAs and CoAs were slowly heated to 1150°C in evacuated silica tubes, and held for 60 hours before cooling down to room temperature at the rate of $50^\circ\text{C}/\text{h}$. The polycrystals were characterized by X-ray diffraction at room temperature and dc magnetization by Quantum Design SQUID. The electrical resistance was measured on sintered pellets with typical four-probe method.

We show the crystal structure of $\text{Ba}(\text{Zn}_{1-2x}\text{Mn}_x\text{Co}_x)_2\text{As}_2$ and the X-ray diffraction patterns in Fig. 1. Bragg peaks from the $\text{Ba}(\text{Zn}_{0.9}\text{Mn}_{0.05}\text{Co}_{0.05})_2\text{As}_2$ can be well indexed by a 122 tetragonal structure, isostructural to the 122 type of Fe-based superconductor $\text{Ba}(\text{Fe}_{1-x}\text{Co}_x)_2\text{As}_2$, as shown in Fig. 1(c). The single phase is conserved with the doping level up to $x = 0.10$. Small traces of non-magnetic Zn_3As_2 impurities appear for higher level of doping. The lattice constant a monotonically increases from $a = 4.120 \text{ \AA}$ for $x =$

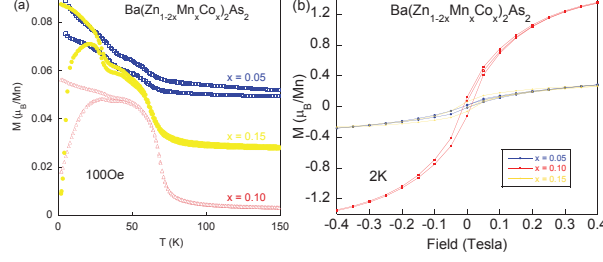


FIG. 2: (Color online) (a) The temperature dependent magnetization M for $\text{Ba}(\text{Zn}_{1-2x}\text{Mn}_x\text{Co}_x)_2\text{As}_2$ with $x = 0.05, 0.10, 0.15$ obtained in the zero field cooling (ZFC) and field cooling (FC) under the external field of 100 Oe. (b) The isothermal magnetization measured at 2 K shows hysteresis loops for this material. The coercive field increases with increasing doping level.

0.05 to 4.145 Å for $x = 0.15$, and c monotonically decrease from $c = 13.605$ Å to 13.554 Å, indicating the successful solid solution of Cr for Zn.

In Fig. 2(a), we show the zero-field cooled (ZFC) and field cooled (FC) measurements of the dc -magnetization M of $\text{Ba}(\text{Zn}_{1-2x}\text{Mn}_x\text{Co}_x)_2\text{As}_2$ ($x = 0.05, 0.10, 0.15$) for $B_{ext} = 100$ Oe. For the doping of $x = 0.05$, we observe a strong increase of M at $T_C = 60$ K, but the splitting between ZFC and FC curves is small. With the doping level increasing to $x = 0.10$, a significant increase in M is observed at the temperature of ~ 75 K, and the ZFC and FC curves split, indicating that ferromagnetic ordering is taking place. T_C decreases to ~ 70 K with the doping level of $x = 0.15$. A close inspection of M indicates that for $x = 0.05$ and 0.10, a step has been observed at $T \sim 30$ K. This is possibly arising from either a spin state change of Co 3d electrons, or the inhomogeneous distribution of Mn or Co atoms in the specimens. We are still working to optimize the synthesis condition and to improve the sample homogeneity. None the less, we believe that either reason does not affect the fact that T_C reaches ~ 80 K at the average doping level of 10 % Mn and Co. We fit the temperature dependence of M above T_C to a Curie-Weiss law. The effective paramagnetic moment is determined to be $2 \sim 3\mu_B/\text{TM}$ (TM = Mn, Co). Currently we do not firmly know if Co introduces spins during the substitution process, and it is difficult to determine the spin state of both Mn and Co. In the p-type DMS mentioned above, Mn ions are of “+2” valence and its high spin state have been demonstrated.

In Fig. 2(b), we show the isothermal magnetization of $\text{Ba}(\text{Zn}_{1-2x}\text{Mn}_x\text{Co}_x)_2\text{As}_2$ ($x = 0.05,$

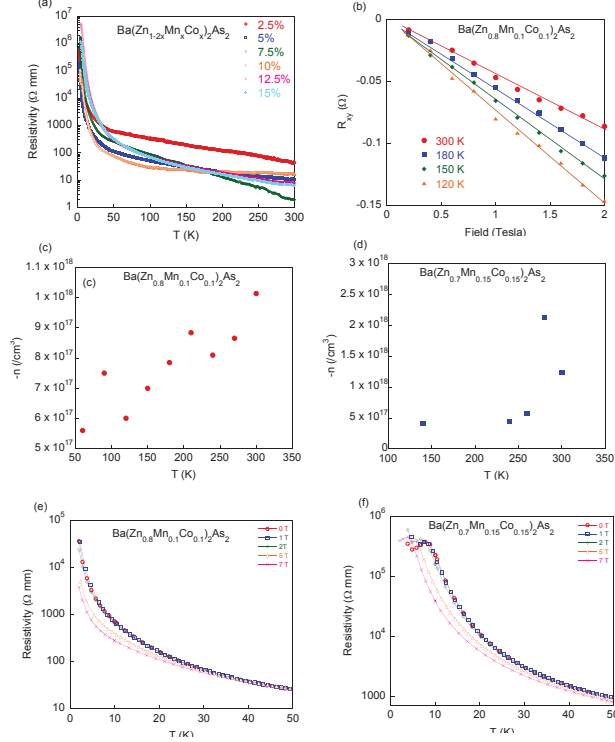


FIG. 3: (Color online) (a) The temperature dependence of resistivity for $\text{Ba}(\text{Zn}_{1-2x}\text{Mn}_x\text{Co}_x)_2\text{As}_2$. (b) Hall resistance of $\text{Ba}(\text{Zn}_{0.8}\text{Mn}_{0.1}\text{Co}_{0.1})_2\text{As}_2$ at 300 K, 180 K, 150 K and 120 K with linear fitting lines. T-dependent carrier density of $\text{Ba}(\text{Zn}_{0.8}\text{Mn}_{0.1}\text{Co}_{0.1})_2\text{As}_2$ (c) and $\text{Ba}(\text{Zn}_{0.7}\text{Mn}_{0.15}\text{Co}_{0.15})_2\text{As}_2$ (d) decreases toward low temperature. The resistivity of $\text{Ba}(\text{Zn}_{0.8}\text{Mn}_{0.1}\text{Co}_{0.1})_2\text{As}_2$ (e) and $\text{Ba}(\text{Zn}_{0.7}\text{Mn}_{0.15}\text{Co}_{0.15})_2\text{As}_2$ (f) under different external fields shows a large magnetic resistance.

0.10, 0.15). For all doping levels, a parallelogram-shaped hysteresis loop with a small coercive field has been observed. For $x = 0.05$, the coercive field at 2 K is 100 Oe. The coercive field continuously increases to 258 Oe with the doping level increasing to 15%. The magnitude of coercive field is comparable to $\sim 50 - 100$ Oe of the cubic structural $\text{Li}_{1.1}(\text{Zn}_{0.97}\text{Mn}_{0.03})\text{As}$ [18], $\text{Li}_{1.1}(\text{Zn}_{0.97}\text{Mn}_{0.03})\text{P}$ [19] and $(\text{Ga}_{0.965}\text{Mn}_{0.035})\text{As}$ [1], but much smaller than the p -type $\text{Ba}_{1-y}\text{K}_y(\text{Zn}_{1-x}\text{Mn}_x)_2\text{As}_2$ [23], which has an identical two dimensional crystal structure.

In Fig. 3(a), we show the electrical resistivity measured for $\text{Ba}(\text{Zn}_{1-2x}\text{Mn}_x\text{Co}_x)_2\text{As}_2$ ($x = 0.025, 0.05, 0.075, 0.10, 0.125, 0.15$). For the parent semiconductor BaZn_2As_2 , the electrical resistivity displays typical semiconducting behavior. Small amount of K doping into Ba sites change it into a metal [23]. In the case of Mn and Co co-doped samples, we found that the resistivity monotonically increases with the decreasing of temperature for all doping levels. The same type of resistive behavior has also been observed in $(\text{Ga}_{1-x}\text{Mn}_x)\text{As}$ for $x \leq 0.03$.

It has been ascribed to the scattering of carriers by magnetic fluctuations through exchange interactions in $(\text{Ga}_{1-x}\text{Mn}_x)\text{As}$ [2]. However, we do not observe insulator to metal transition when the doping level reaches as high as 15%.

We have also conducted the Hall effect measurements for the sample of $\text{Ba}(\text{Zn}_{1-2x}\text{Mn}_x\text{Co}_x)_2\text{As}_2$ ($x = 0.10$ and 0.15), and show the data in Fig. 3(b)-(d). Our results indicate that the carriers are *n*-type, with an electron density in the order of $n \sim 5 \times 10^{17} \text{ cm}^{-3}$. This carrier density is comparable to that of $\text{Li}_{1.1}\text{Zn}_{1-x}\text{Mn}_x\text{P}$ [19] and II-VI DMSs. In the research of Fe-based high temperature superconductors, Co substitution for Fe in BaFe_2As_2 introduce electrons, and superconductivity with $T_c \sim 25 \text{ K}$ has been achieved. It has been shown by ARPES (angle-resolved photoemission spectroscopy) that sufficient amount of Co doping kills the hole Fermi surfaces [25] residing in the center of the Brillion zone, and expand the electron Fermi surfaces [25]. The *n*-type carriers in $\text{Ba}(\text{Zn}_{1-2x}\text{Mn}_x\text{Co}_x)_2\text{As}_2$ should be attributed to the Co substitution for Zn. We also measured the magneto-resistance (MR) for the doping level of $x = 0.10$ and 0.15 . Under the magnetic field of 7 Tesla, the magnitude of electrical resistivity at 2 K decrease -89% and -78% for $x = 0.10$ and 0.15 samples, respectively. The negative magnetoresistance can be attributed to the reduction of disorders among the local spins, and the followed suppression of magnetic scattering by external field.

In diluted magnetic systems, the magnetic impurities can easily give rise to spurious features of “ferromagnetism”, such as the bifurcation of ZFC and FC curves and hysteresis loops [26, 27]. In the $\text{Ba}(\text{Zn}_{1-2x}\text{Mn}_x\text{Co}_x)_2\text{As}_2$ system, the ordering temperature T_C systematically changes with the variation of Mn and Co doping levels, indicating that the magnetic ordering is truly arising from the Mn and Co atoms that substituted for the Zn atoms in ionic sites. We would observe a single transition temperature for all doping levels if the magnetic ordering arises from the same type of magnetic impurity source. μSR technique is a powerful tool to determine the magnetic ordered volume at a microscopic level, as has been demonstrated in the bulk form p-type DMS materials [18, 20, 23]. We have also conducted μSR measurement of the $\text{Ba}(\text{Zn}_{1-2x}\text{Mn}_x\text{Co}_x)_2\text{As}_2$, and our preliminary μSR results on 15% doped specimen indicate that static ferromagnetic ordering do develops at low temperature.

On the other hand, the bifurcation of ZFC and FC curves and the hysteresis loops can be found not only in regular ferromagnets [28] but also in spin glasses [29]. The saturation moment reach $\sim 1 \mu_B/\text{TM}$ (TM = Mn, Co) in $\text{Ba}(\text{Zn}_{1-2x}\text{Mn}_x\text{Co}_x)_2\text{As}_2$ under the field of

0.4 Tesla. The ground state is not likely a spin glass state because the saturation moment of a spin glasses is usually in the order of $0.01 \mu_B/\text{Mn}$ or even smaller. Experimental, neutron scattering can resolve spatial spin correlations, and is a decisive technique to distinguish the two cases. We have conducted neutron diffraction experiment on $(\text{Ba}_{0.7}\text{K}_{0.3})(\text{Zn}_{0.9}\text{Mn}_{0.1})_2\text{As}_2$ [23] and $(\text{La}_{0.9}\text{Sr}_{0.1})(\text{Zn}_{0.9}\text{Mn}_{0.1})\text{AsO}$ [30] polycrystalline DMS specimens which have a much larger saturation moment size, $\sim 0.4 - 1 \mu_B/\text{Mn}$. Unfortunately, it is still difficult to decouple the magnetic and structural Bragg peaks even at 6 K due to the spatially dilute Mn moments [31]. For the n-type $\text{Ba}(\text{Zn}_{1-2x}\text{Mn}_x\text{Co}_x)_2\text{As}_2$ system, it will be easier to grow single crystals since Mn and Co are more easily to alloy with Zn. Upon the single crystals are available, high resolution neutron scattering experiments will be conducted.

Several theoretical models has been proposed to explain the ferromagnetism in various diluted magnetic semiconductors and oxides, such as Zener's model [32], percolation of bound magnetic polarons (BMPs) [33–35], and $d-d$ double exchange due to hopping between transition metal d states [36]. In the case of $\text{Ba}(\text{Zn}_{1-2x}\text{Mn}_x\text{Co}_x)_2\text{As}_2$, the resistivity is very large ($\sim 10^5 \Omega \text{ mm}$) and the carrier density is as low as $\sim 10^{17} \text{ cm}^{-3}$. The origin of the ferromagnetism seems more amenable with the BMPs model.

In summary, we reported the synthesis and characterization of bulk form diluted magnetic semiconductors $\text{Ba}(\text{Zn}_{1-2x}\text{Mn}_x\text{Co}_x)_2\text{As}_2$ with the ordering temperature as high as $\sim 80 \text{ K}$. It is the first time that Mn and Co atoms are co-doped into the BaZn_2As_2 semiconductor and a ferromagnetic ordering is observed. The Hall effect measurements indicate that the carrier is n -type with a density in the order of $10^{17}/\text{cm}^{-3}$. The magneto-resistance reaches to $\sim -89\%$ under the external field of 7 Tesla. Finally, we would like to emphasize that the common crystal structure and excellent lattice matching between the p-type ferromagnetic $\text{Ba}_{1-y}\text{K}_y(\text{Zn}_{1-x}\text{Mn}_x)_2\text{As}_2$, the n-type ferromagnetic $\text{Ba}(\text{Zn}_{1-2x}\text{Mn}_x\text{Co}_x)_2\text{As}_2$, the antiferromagnetic BaMn_2As_2 and the superconducting $\text{Ba}(\text{Fe}_{1-x}\text{Co}_x)_2\text{As}_2$ systems make it possible to make various junctions between these systems through the As layer.

The work at Zhejiang University was supported by National Basic Research Program of China (No. 2011CBA00103, No. 2014CB921203), NSFC (No. 11274268); F.L. Ning acknowledges helpful discussion with C.Q. Jin and Y.J. Uemura.

-
- [1] H. Ohno, A. Shen, F. Matsukura, A. Oiwa, A. Endo, S. Katsumoto, and Y. Iye, Appl. Phys. Lett. **69**, 363 (1996).
 - [2] T. Jungwirth, J. Sinova, J. Masek, J. Kucera, and A.H. MacDonald, Rev. Mod. Phys. **78**, 809 (2006).
 - [3] T. Dietl, Nature Materials **9**, 965 (2010).
 - [4] I. Zutic, J. Fabian, and S. Das Sarma, Rev. Mod. Phys. **76**, 323 (2004).
 - [5] L. Chen, S. Yan, P.F. Xu, W.Z. Wang, J.J. Deng, X. Qian, Y. Ji, and J.H. Zhao, Appl. Phys. Lett. **95**, 182505 (2009).
 - [6] L. Chen, X. Yang, F.H. Yang, J.H. Zhao, J. Misuraca, P. Xiong, and S.V. Molnar, Nano Lett. **11**, 2584 (2011).
 - [7] M. Dobrowolska, K. Tivakornsasithorn, X. Liu, J.K. Furdyna, M. Berciu, K.M. Yu, and W. Waluliewicz, Nature Materials **11**, 444 (2012).
 - [8] A. Pajczkowska, Prog. Cryst. Growth Charact. **1**, 289 (1978).
 - [9] J.K. Furdyna, J. Appl. Phys. **64**, R29 (1988).
 - [10] T. Wojtowicz, T. Dietl, M. Sawicki, W. Plesiewicz, and J. Jaroszynski, Phys. Rev. Lett. **56**, 2419 (1986).
 - [11] H. Morkoç, S. Strite, G. B. Gao, M. E. Lin, B. Sverdlov, and M. Burns, J. Appl. Phys. **76**, 1363 (1994).
 - [12] P.M. Shand, A.D. Christianson, T.M. Pekarek, L.S. Martinson, J.W. Schweitzer, I. Miotkowski, and B.C. Crooker, Phys. Rev. B **58**, 12876 (1998).
 - [13] J. Masek, J. Kudrnovsky, F. Maca, B.L. Gallagher, R.P. Campion, D.H. Gregory, and T. Jungwirth, Phys. Rev. Lett. **98**, 067202 (2007).
 - [14] R. Bacewicz, and T.F. Ciszek, Appl. Phys. Lett. **52**, 1150 (1988).
 - [15] K. Kuriyama, and F. Nakamura, Phys. Rev. B **36**, 4439 (1987).
 - [16] K. Kuriyama, T. Kato, and K. Kawada, Phys. Rev. B **49**, 11452 (1994).
 - [17] S.H. Wei, and A. Zunger, Phys. Rev. Lett. **56**, 528 (1986).
 - [18] Z. Deng, C.Q. Jin, Q.Q. Liu, X.C. Wang, J.L. Zhu, S.M. Feng, L.C. Chen, R.C. Yu, C. Arguello, T. Goko, F.L. Ning, J.S. Zhang, Y.Y. Wang, A.A. Aczel, T. Munsie, T.J. Williams,

- G.M. Luke, T. Kakeshita, S. Uchida, W. Higemoto, T.U. Ito, B. Gu, S. Maekawa, G.D. Morris, and Y.J. Uemura, *Nature Communications* **2**, 422 (2011).
- [19] Z. Deng, K. Zhao, B. Gu, W. Han, J.L. Zhu, X.C. Wang, X. Li, Q.Q. Liu, R.C. Yu, T. Goko, B. Frandsen, L. Liu, J.S. Zhang, Y.Y. Wang, F.L. Ning, S. Maekawa, Y.J. Uemura, and C.Q. Jin, *Phys. Rev. B* **88**, 081203(R) (2013).
- [20] C. Ding, H.Y. Man, C. Qin, J.C. Lu, Y.L. Sun, Q. Wang, B.Q. Yu, C.M. Feng, T. Goko, C.J. Arguello, L. Liu, B.A. Frandsen, Y.J. Uemura, H.D. Wang, H. Luetkens, E. Morenzoni, W. Han, C.Q. Jin, T. Munsie, T.J. Williams, R.M. DOrtenzio, T. Medina, G.M. Luke, T. Imai, and F.L. Ning, *Phys. Rev. B* **88**, 041102(R) (2013).
- [21] W. Han, K. Zhao, X.C. Wang, Q.Q. Liu, F.L. Ning, Z. Deng, Y. Liu, J.L. Zhu, C. Ding, and C.Q. Jin, *Science China-Physics, Mechanics, Astronomy* **56**, 2026 (2013).
- [22] X.J. Yang, Y.K. Li, C.Y. Shen, B.Q. Si, Y.L. Sun, Q. Tao, G.H. Cao, Z.A. Xu, and F.C. Zhang, *Appl. Phys. Lett.* **103**, 022410 (2013).
- [23] K. Zhao, Z. Deng, X.C. Wang, W. Han, J.L. Zhu, x. Li, Q.Q. Liu, R.C. Yu, T. Goko, B. Frandsen, L. Liu, F.L. Ning, Y.J. Uemura, H. Dabkowska, G.M. Luke, H. Luetkens, E. Morenzoni, S.R. Dunsiger, A. Senyshyn, P. Böni, and C.Q. Jin, *Nature Communications* **4**, 1442 (2013).
- [24] X.J. Yang, Y.K. Li, P. Zhang, Y.K. Luo, Q. Chen, C.M. Feng, C. Cao, J.H. Dai, Q. Tao, G.H. Cao, and Z.A. Xu, *J. Appl. Phys.* **114**, 223905 (2013).
- [25] G.R. Stewart, *Rev. Mod. Phys.* **83**, 1589 (2011).
- [26] N. Samarth, *Nature Materials* **9**, 955 (2010).
- [27] S. Chambers, *Nature Materials* **9**, 956 (2010).
- [28] N.W. Ashcroft, and N.D. Mermin, *Solid State Physics* (Holt, Rinehart and Winston, 1976).
- [29] K.H. Fischer, and J.A. Hertz, *Spin Glasses* (Cambridge University Press, 1991).
- [30] J.C. Lu, H.Y. Man, C. Ding, Q. Wang, B.Q. Yu, S.L. Guo, Y.J. Uemura, W. Han, C.Q. Jin, H.D. Wang, B. Chen, and F.L. Ning, *Europhysics Letters* **103**, 67011 (2013).
- [31] F.L. Ning, Y. Zhao et al., to be submitted.
- [32] T. Dietl, H. Ohno, F. Matsukura, J. Cibert, and D. Ferrand, *Science* **287**, 1019 (2000).
- [33] M. Berciu, and R.N. Bhatt, *Phys. Rev. Lett.* **87**, 107203 (2001).
- [34] A. Kaminski, and S.D. Sarma, *Phys. Rev. Lett.* **88**, 247202 (2002).
- [35] J.M.D. Coey, M. Venkatesan, and C.B. Fitzgerald, *Nat. Mater.* **4**, 173 (2005).
- [36] A.J. Millis, *Nature* **392**, 147 (1998).